Complex Functional Systems with Three Different Types of Dynamic Covalent Bonds

Zhang, Kangda; Matile, Stefan

How to cite

ZHANG, Kangda, MATILE, Stefan. Complex Functional Systems with Three Different Types of Dynamic Covalent Bonds. In: Angewandte Chemie. International edition in English, 2015, vol. 54, n° 31, p. 8980–8983. doi: 10.1002/anie.201503033

This publication URL: https://archive-ouverte.unige.ch/unige:74454
Publication DOI: 10.1002/anie.201503033

Complex Functional Systems with Three Different Types of Dynamic Covalent Bonds

Kang-Da Zhang,[a] and Stefan Matile[a]*

[a] Dr. K.-D. Zhang, Prof. S. Matile

Department of Organic Chemistry

University of Geneva, Geneva, Switzerland

Fax: (+) 41 22 379 3215

E-mail: stefan.matile@unige.ch

Homepage: www.unige.ch/sciences/chiorg/matile/

Supporting information for this article is given via a link at the end of the document.

Abstract: In this report, we introduce multicomponent surface architectures that operate with three different dynamic covalent bonds. Disulfide exchange under basic conditions accounts for the growth of π-stacks on solid surfaces. Hydrazone exchange under acidic conditions is used to add a second co-axial string or stack, and boronic ester exchange under neutral conditions to co-align a third one. The newly introduced boronic ester exchange chemistry is compatible with stack and string exchange without interference from the orthogonal hydrazone and disulfide exchange. The functional relevance of surface architectures with three different dynamic covalent bonds is exemplified with the detection of polyphenol natural products such as epigallocatechin gallate in competition experiments with alizarin red. These results describe synthetic strategies to create functional systems of unprecedented sophistication with regard to dynamic covalent chemistry.

Dynamic covalent bonds are fascinating because of their dual nature.[1,2] Under some conditions, they are as rapidly reversible as non-covalent bonds, under different conditions, they

exist as irreversibly as covalent bonds. This dual nature is of decisive importance to build "living" functional systems that can self-sort, self-heal, adapt, template, amplify, exchange, replicate, transcribe, sense, walk, penetrate cells and respond to a broad spectrum of physical and chemical stimulation, including light.[1,2] Synthetic methods that employ a single type of dynamic covalent bonds to create function are very well developed.[1] In sharp contrast, only a few pioneering examples exist for two types of dynamic covalent bonds that work together.[2] Best developed is the combination of disulfide exchange under basic and hydrazone exchange under acidic conditions,[2-6] promising alternatives include boronic ester,[7-10] thioester,[11] amide,[11,12] imine[8,13-15] and hemiaminal exchange,[16] Michael adducts,[17] olefin metathesis[15] and Cope rearrangements.[9] Functional systems that employ more than two organic dynamic covalent bonds together have not been reported so far. Attempts to also integrate inorganic coordination chemistry into systems with more than two dynamic covalent bonds have focused mostly on structural aspects.[18] The rare use of more than one organic dynamic covalent bond in concert is surprising because non-covalent bonds are routinely used together to build complex functional systems.[2] Here we report multicomponent surface architectures that are built with three different types of dynamic covalent bonds.

The construction of multicomponent surface architectures with three different types of dynamic covalent bonds was based on the recently introduced SOSIP-TSE methodology.[5,6] Oriented π-stacks of naphthalenediimides (NDIs) were grown directly on indium tin oxide (ITO) surfaces by self-organizing surface-initiated polymerization (SOSIP). This established method operates with ring-opening disulfide-exchange chemistry under basic conditions. To facilitate reading, we marked building blocks used for disulfide exchange with an **S**, hydrazone exchangers with **H**, boronic ester exchangers with **B**, and the resulting surface architectures as the respective combination (Figure 1). In architecture **S1H1** obtained by SOSIP,[5,6] the

individual NDI stacks are separated by NDI templates on the surface and benzaldehyde templates **H1** along the stack. The substitution of **H1** in **S1H1** by hydrazone exchange under acidic conditions has been referred to as TSE, i.e. templated stack exchange (or string exchange in the absence of clear stacks).[5,6] TSE is a two step process composed of templated stack or string release (TSR) followed by templated stack or string addition (TSA).

TSR of aldehyde **H1** from surface architectures **S1H1** was achieved by dipping the ITO electrodes in aqueous solutions of hydroxylamine (Figure 1).[5,6] The formation of surface architectures **S1** was followed by changes in the absorbance of the transparent ITO electrodes as described (Figure S1).[5,6] For TSA, the hydrazides produced along the NDI stacks in surface architecture **S1** were then reacted under acidic conditions with aldehydes containing an additional boronic acid, e.g. **H2** or **H3**. According to changes in the absorbance of the ITO electrodes, TSE from **S1H1** to **S1H2**, **S1H3**, etc, was general and occurred in quantitative yield (Figure S1). A focused screening of different boronic acids identified **H2** and the newly synthesized,[19] formylated benzoboroxole or benzoxaborole[19] **H3** as best. Among other boronic acids tested, the ones in *ortho* position to aldehydes[7,8] were less performant, presumably because of unfavorable topology and direct dependence of boronic ester exchange on hydrazone exchange.

Boronic ester formation of alizarin red **B1**[20] in solution shifts the broad absorption maximum of the chromophore from λ_{max} = 530 nm to λ_{max} = 460 nm (Figure 2a). Apparent dissociation constants in MeOH/water 3:1 increased from **H3** (K_D = 1.46 mM) to **H2** (K_D = 90 μM, Table 1, entries 3 and 4). Incubation of **S1H3** with a solution of **B1** in DMSO containing 2% Hünig's base afforded an ITO electrode with strong absorbance at λ_{max} ~ 465 nm (Figure 2b). Confirming the formation of boronic esters, the appearance of this band was consistent with the formation of **S1H3B1** (Figure 1).

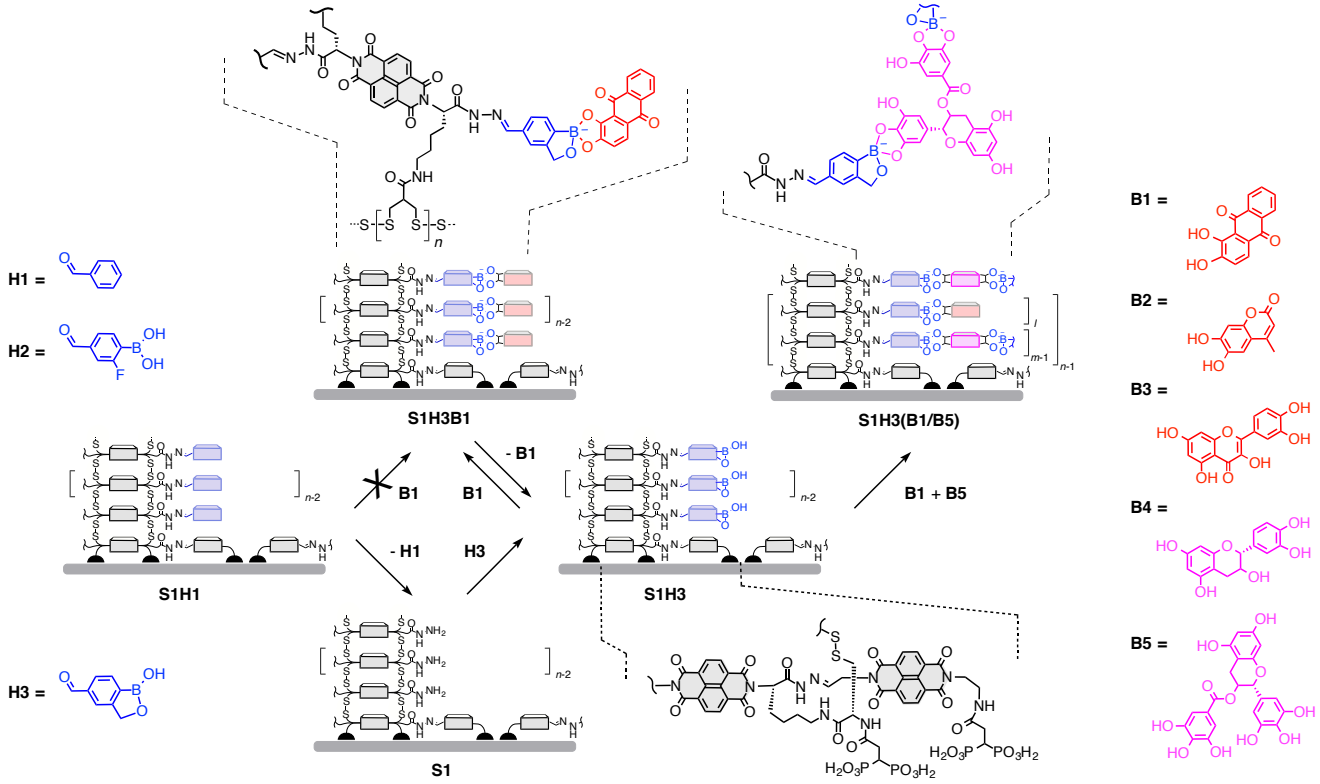

Figure 1. Schematic structures of representative surface architectures **S1H3B1** and **S1H3(B1/B5)** with dynamic covalent disulfides, hydrazones and boronic esters, with synthesis from **S1H1** and molecular structure of all hydrazone (**H1**-**H3**) and boronic ester exchangers (**B1**-**H5**).

Dose response curves revealed that complete TSA to **S1H3** occurs with concentrations of **B1** down to ~ 3 mM (Figure 3a). The EC_{50}, that is the concentration needed to observe 50% of the maximal TSA, was found at EC_{50} = 620 μM (Table 1, entry 4). The same dose response curve gave a maximal yield η_{MAX} = 92% for the construction of **S1H3B1** (Figure 3a, Table 1, entry 4). Control experiments showed that TSA of **B1** does not occur with **S1H1**, i.e. in the absence of boronic acids (Figures 1, S10, Table 1, entry 2), and that **S1H3** is not affected under these mildly basic conditions for the time needed for TSA, i.e., disulfides and hydrazones remain intact during boronic ester exchange.

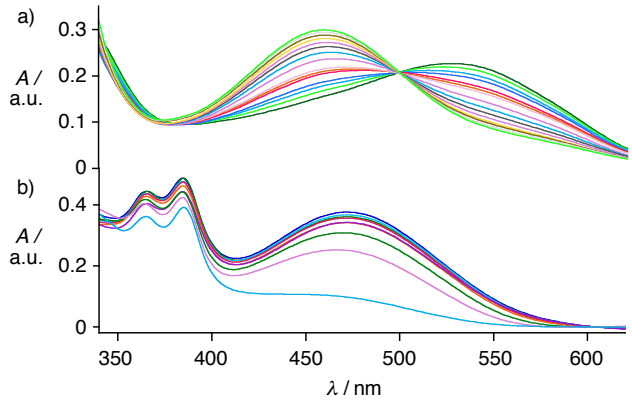

Figure 2. a) Absorption of **B1** (43 µM) in 75% MeOH, 100 mM HEPES, pH 7.8, in the presence of increasing concentrations of **H3** (0-50 mM, 460 nm, ↑; 530 nm, ↓). b) Absorption of **S1H3** after incubation with increasing concentrations of **B1** in DMSO (2% Hünig's base, 0.4 - 100 mM, ~465 nm, ↑).

TSA of **B1** or coumarin[20] **B2** to **S1H2** or **S1H3** in DMSO with 2% Hünig's base occurred with η_{MAX} > 75%, while TSA in DMSO/water 8:2 gave η_{MAX} = 34-49% only (Table 1, entries 3-6, Figures S6-S9). Under the best conditions, TSA with quercetin **B3** gave only η_{MAX} = 49% for both **S1H2B3** and **S1H3B3** (Table 1, entries 7 and 8). This poor yield could indicate that **B3** forms esters with two proximal boronic acids in the confined space of the surface architectures (Ongoing studies with multivalent chromophores strongly support this interpretation). For **B1**-**B3**, the EC_{50}'s with **S1H3** were better than with **S1H2**, although K_D's with **H3** in solution were weaker than with **H2** (Table 1, entries 3-8). This finding confirmed previous observations[21] that the chemistry on surfaces, dominated by powerful proximity effects in confined space, and chemistry in solution are not the same. Further studies focused mostly on **S1H3** because of these impressive EC_{50}'s.

Table 1. Characteristics of Surface Architectures.

	System [a]	η_{MAX} / % [b-e]	EC_{50} / mM [f-h]	K_D / mM [i]	t_{50} / s [j]
1	**S1H2**	99[b]	~10	-	$>10^5$
2	**S1H1B1**	0[c]	-	-	-
3	**S1H2B1**	87[c] / 49[d]	12[f]	0.09	976
4	**S1H3B1**	92[c] / 44[d]	0.62[f]	1.46	233
5	**S1H2B2**	97[c] / 34[d]	1.3[f]	0.03	201
6	**S1H3B2**	76[c] / 35[d]	0.56[f]	4.20	43
7	**S1H2B3**	49[c] / 17[d]	15[f]	0.17	65
8	**S1H3B3**	49[c] / 22[d]	1.3[f]	1.04	27
9	**S1H3B4**	100[e]	76[g] / 22[h]	-	-
10	**S1H3B5**	66[e]	4.6[g] / 2.1[h]	-	-
11	**S1H3B6**	100[e]	-[g] / 5.1[h]	-	-

[a]See Figure 1 for structures, **B6** = polyphenon 60, a commercially available green tea extract. [b-e] Maximal yields for TSA and TSE, estimated from dose response curves based on changes in absorbance of the ITO electrodes (e.g., Figure 2b, 3a). Comparison with absorption spectra measured in solution after full destruction with mercaptoethanol indicated that, compared to the nearly environment insensitive NDI absorption,[5,6] the extinction coefficients of the chromophores used to follow boronic ester exchange do not change much in surface architectures either, i.e., the accuracy of yields estimated directly from the absorbance of the ITO electrodes is reasonable. [b]TSE with hydrazones (4% AcOH).[5,6] [c]TSA in DMSO (2% Hünig's base). [d] TSA in 80% DMSO, pH 7.4. [e]From co-TSA with **B1**. [f-h]Half maximal effective (EC_{50})[f] or inhibitory (IC_{50})[g,h] concentrations, i.e. the concentrations needed to reach $\eta_{MAX}/2$. [f]EC_{50} in mM (Figures 2b and 3a). [g]IC_{50} for inhibition of **S1H3B1**, in mM. [h]Same in mg mL^{-1} (Figure 3d). [i]Dissociation constants of boronic esters **HxBx** in solution (75% MeOH, 100 mM HEPES, pH 7.8, Figure 2a). [j]Lifetime in wet DMSO (Figure 3b).

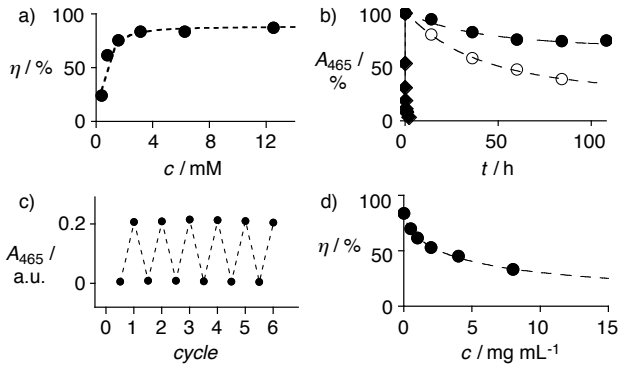

Figure 3. a) TSA yields for **S1H3B1** as a function of the concentration *c* of **B1** during incubation of **S1H3** in DMSO (2% Hünig's base) (from Figure 2b, with Hill analysis). b) Absorption at λ = 465 nm as a function of incubation time of **S1H3B1** in wet DMSO (◆), dry DMSO (○) and dry toluene (●). c) Reversibility of TSR from **S1H3B1** (Figure 3b) and TSA to **S1H3** (Figure 2b, with 100 mM **B1**). d) TSA yields for **S1H3B1** as a function of the concentration *c* of green tea extract **B6** during incubation of **S1H2** in DMSO (2% Hünig's base, 3.1 mM **B1**, from Figure S17b).

With evidence for the generality of TSA by boronic ester formation in hand, TSE was explored next. TSR of **B1** from **S1H3B1** occurred spontaneously upon incubation in any solution containing water (Figure 3b, ◆). In wet DMSO, the half live t_{50} of the surface architectures increased from **S1H3Bx** to **S1H2Bx** (Table 1, entries 3-8, Figures S12, S13) and with pH (Figures S14, S15), i.e., with the stability of the boronic ester. In dry DMSO, TSR rates became very slow (Figure 3b, ○, S16a). In dry toluene, surface architectures were stable for many days except for a minor initial decrease, possibly due to traces of water (Figure 3b, ●, S16b). TSR and TSA could be repeated without losses in yield, simply by dipping **S1H3** into solutions with and without **B1,** i.e., TSE by boronic ester exchange is unproblematic, also in the presence of disulfides and hydrazones (Figure 3c).

Co-TSA was explored by incubation of **S1H3** with increasing concentrations of catechin **B4** in DMSO containing 2% Hünig's base and 3.1 mM **B1**. Decreasing absorption at λ_{max} = 465 nm was observed (Figure S17a). Dose response curves gave an IC_{50} = 76 mM for the inhibition of **B1** addition by **B4**. This finding demonstrated that with increasing concentrations of **B4** at constant **B1**, the composition of the produced surface architectures changes from red **S1H3B1** over mixed architectures **S1H3(B1/B4**) to the colorless **S1H3B4** (Table 1, entry 9). Complete inhibition of TSA of **B1** with **B4** at higher concentrations demonstrated that the synthesis of **S1H3B4** is quantitative, i.e., η_{MAX} = 100% (Table 1, entry 9). For epigallocatechin gallate **B5**, another major polyphenol in green tea, IC_{50} = 4.6 mM and η_{MAX} = 66% were found under the same conditions (Figure S17c, Table 1, entry 10). High activity and incomplete co-TSA were both consistent with the large size and the multivalency of **B5** (Figure 1).[7] Polyphenon 60 **B6**, a green tea extract, inhibited TSA of **B1** to **S1H3** with an IC_{50} = 5.1 mg mL^{-1} (Figure 3d, Table 1, entry 11). This intermediate activity was very meaningful considering that the weaker catechin **B4** and the stronger epigallocatechin gallate **B5** are the main polyphenols present in green tea. Compatibility of dose response curves for polyphenon 60 with enzymatic signal generation for polyphenol sensing applications with has been demonstrated previously in a different context.[7]

Taken together, these results demonstrate existence and functional relevance of multicomponent architectures that operate with three different dynamic covalent bonds, here disulfides, hydrazones and boronic esters. Possible applications are diverse, directionality and compatibility with optoelectronic signal generation, transduction and detection, interfacing and device fabrication appear particularly advantageous.[5-7,22,23] With regard to synthetic methods development, the next milestones will concern the integration of self-sorting[7b,c] and fully

independent dynamics for three orthogonal dynamic covalent bonds, and, last but not least, the introduction of the fourth orthogonal dynamic covalent bond.

Acknowledgements

We thank Davide Bonifazi (Namur) for discussions, the NMR and the Sciences Mass Spectrometry (SMS) platforms for services, and the University of Geneva, the European Research Council (ERC Advanced Investigator), the Swiss National Centre of Competence in Research (NCCR) Molecular Systems Engineering, the Swiss NCCR Chemical Biology and the Swiss NSF for financial support.

Keywords: Dynamic covalent bonds • complex functional systems • boronic esters • hydrazones • disulfides

[1] a) X. Wu, Z. Li, X.-X. Chen, J. S. Fossey, T. D. James, Y.-B. Jiang, *Chem. Soc. Rev.* **2013**, *42*, 8032-8048; b) S. Zarra, D. M. Wood, D. A. Roberts, J. R. Nitschke, *Chem. Soc. Rev.* **2015**, *44*, 419-432; c) A. Herrmann, *Chem. Soc. Rev*. **2014**, *43*, 1899-1933; d) J. Li, P. Nowak, S. Otto, *J. Am. Chem. Soc.* **2013**, *135*, 9222-9239; e) S. P. Black, J. K. M. Sanders, A. R. Stefankiewicz, *Chem. Soc. Rev.* **2014**, *43*, 1861-1872; f) J.-M. Lehn, *Top. Curr. Chem*. **2012**, *322*, 1-32; g) S. J. Rowan, S. J. Cantrill, G. R. L. Cousins, J. K. M. Sanders, J. F. Stoddart, *Angew. Chem.* **2002**, *114*, 938–993; *Angew. Chem. Int. Ed.* **2002**, *41*, 899-952; h) Y. Jin, C. Yu, R. J. Denman. W. Zhang, *Chem. Soc. Rev.* **2013**, *42*, 6634-6654.

[2] A. Wilson, G. Gasparini, S. Matile, *Chem. Soc. Rev.* **2014**, *43*, 1948-1962.

[3] M. J. Barrell, A. G. Campaña, M. von Delius, E. M. Geertsema, D. A. Leigh, *Angew. Chem.* **2011**, *123*, 299-304; *Angew. Chem. Int. Ed*. **2011**, *50*, 285-290.

[4] G. Deng, F. Li, H. Yu, F. Liu, C. Liu, W. Sun, H. Jiang, Y. Chen, *ACS Macro Lett*. **2012**, *1*, 275-279.

[5] N. Sakai, S. Matile, *J. Am. Chem. Soc.* **2011**, *133*, 18542-18545.

[6] a) H. Hayashi, A. Sobczuk, A. Bolag, N. Sakai, S. Matile, *Chem. Sci.* **2014**, *5*, 4610-4614; b) M. Lista, J. Areephong, N. Sakai, S. Matile, *J. Am. Chem. Soc.* **2011**, *133*, 15228-15231; c) E. Orentas, M. Lista, N.-T. Lin, N. Sakai, S. Matile, *Nat. Chem.* **2012**, *4*, 746-750.

[7] a) S. Hagihara, H. Tanaka, S. Matile, *J. Am. Chem. Soc.* **2008**, *130*, 5656-5657; b) A. Hennig, S. Matile, *Chirality* **2009**, *21*, 826-835.

[8] a) Y. Perez-Fuertes, A. M. Kelly, A. L. Johnson, S. Arimori, S. D. Bull, T. D. James, *Org. Lett.* **2006**, *8*, 609-612; b) D. A. Tickell, M. F. Mahon, S. D. Bull, T. D. James, *Org. Lett.* **2013**, *15*, 860-863.

[9] J. F. Teichert, D. Mazunin, J. W. Bode, *J. Am. Chem. Soc.* **2013**, *135*, 11314-11321.

[10] a) G. Zhang, O. Presly, F. White, I. M. Oppel, M. Mastalerz, *Angew. Chem.* **2014**, *126*, 5226-5230; *Angew. Chem. Int. Ed.* **2014**, *53*, 5126-5130; b) B. Icli, E. Solari, B. Kilbas, R. Scopelliti, K. Severin, *Chem. Eur. J.* **2012**, *18*, 14867-14874; c) S. L. Wiskur, E. V. Anslyn, *J. Am. Chem. Soc.* **2001**, *123*, 10109-10110.

[11] N. Ollivier, J. Vicogne, A. Vallin, H. Drobecq, R. Desmet, O. El Mahdi, B. Leclercq, G. Goormachtigh, V. Fafeur, O. Melnyk, *Angew. Chem.* **2012**, *124*, 213-217; *Angew. Chem. Int. Ed.* **2012**, *51*, 209-213.

[12] N. Ruff, V. Garavini, N. Giuseppone, *J. Am. Chem. Soc.* **2014**, *136*, 6333-6339.

[13] J. W. Sadownik, D. Philp, *Angew. Chem.* **2008**, *120*, 10113-10118; *Angew. Chem. Int. Ed.* **2008**, *47*, 9965-9970.

[14] Y. Zeng, R. Zou, Z. Luo, H. Zhang, X. Yao, X. Ma, R. Zou, Y. Zhao, *J. Am. Chem. Soc.* **2015**, *137*, 1020-1023.

[15] a) K. D. Okochi, Y. Jinz, W. Zhang, *Chem. Commun.* 2013, 49, 4418-20; b) K. D. Okochi, G. S. Han, I. M. Aldridge, Y. Liu, W. Zhang, *Org. Lett.* **2013**, *15*, 4296-4299.

[16] H. H. Jo, R. Edupuganti, L. You, K. N. Dalby, E. V. Anslyn, *Chem. Sci.* **2015**, *6*,158-164.

[17] A. G. Campaña, D. A. Leigh, U. Lewandowska, *J. Am. Chem. Soc.* **2013**, *135*, 8639-8645.

[18] a) R. J. Sarma, S. Otto, J. R. Nitschke, *Chem. Eur. J.* **2007**, *34*, 9542-9546; b) M. D. Wise, J. J. Holstein, P. Pattison, C. Besnard, E. Solari, R. Scopelliti, G. Bricogne, K. Severin, *Chem. Sci.* **2015**, *6*, 1004-1010.

[19] a) M. Bérubé, M. Dowlut, D. G. Hall, *J. Org. Chem.* **2008**, *73*, 6471-6479; b) G. A. Ellis, M. J. Palte, R. T. Raines, *J. Am. Chem. Soc.* **2012**, *134*, 3631-3634.

[20] L. Zhu, Z. Zhong, E. V. Anslyn, *J. Am. Chem. Soc.* **2005**, *127*, 4260-4269.

[21] A. Carmine, Y. Domoto, N. Sakai, S. Matile, *Chem. Eur. J.* **2013**, *19*, 11558-11563.

[22] H. H. Jo, C. Y. Lin, E. V. Anslyn, *Acc. Chem. Res.* **2014**, *47*, 2212-2221.

[23] T. Takeuchi, S. Matile, *Chem. Commun.* **2013**, *49*, 19-29.